Mean-Field Phase Diagrams of a Random Uniaxial Heisenberg Ferromagnet

M. N. Tamashiro and S. R. A. Salinas

Instituto de Física, Universidade de São Paulo,

Caixa Postal 20516, São Paulo, CEP 01498-970, SP, Brasil

Received August 28, 1992

We use mean-field techniques to obtain the global phase diagrams for a classical Heisenberg model in the presence of random uniaxial single-ion anisotropic terms. For a diluted anisotropy, the phase diagrams do not display an oblique phase. As in the pure case, the Ising and XY ordered phases are separated by a first-order line which ends at a bicritical point. For a competitive and symmetric double-delta distribution, the phase diagrams display an oblique phase and the possibility of two distinct multicritical points. Introducing n replicas of the short-range model, we perform some preliminary renormalization-group calculations to first order in $\varepsilon = 4 - d$. In the $n \to 0$ limit, however, there is only a single stable fixed point which cannot be reached from physically acceptable conditions.

I. Introduction

The therrnodynamic behavior of many insulating antiferromagnetic compounds can be described by a uniaxial Heisenberg model, given by the spin Hamiltonian

$$\mathcal{H} = J \sum_{(i,j)} \mathbf{S}_i \cdot \mathbf{S}_j - D \sum_{i=1}^{N} (S_i^z)^2 - H \sum_{i=1}^{N} S_i^z, \qquad (1.1)$$

where J > 0, D is the parameter of anisotropy, H is the applied field along the easy axis, the first sum is over nearest neighbors of a crystal lattice, and $\mathbf{S}_i$ is a classical three-dimensional vector on site i. There are some experiments on quenched random mixtures of isomorphous antiferromagnets with distinct rnagnetic orderings. For instance, mixtures of $MnBr_2.4H_2O$ and $MnCl_2.4H_2O$[1,2] still keep the same crystalline structure, although the atoms of chlorine and bromine are assigned at rsndom to the lattice positions. As the easy axes of the pure compounds are approximately parallel, the field-temperature phase diagram of the mixture still displays a flop line which ends at a bicritical point. Another interesting example are mixtures of $FeCl_2.2H_2O$ and $CoCl_2.2H_2O$[3,4]. In this case, the easy axes of the pure compounds are almost perpendicular. The phsse diagrams of the mixtures can then display an oblique intermediate phase and a tetracritical point. As a first approximation, the critica1 behavior of these mixed compounds can be understood in terms of a random-anisotropy Hamiltonian,

$$\mathcal{H} = J \sum_{(i,j)} \mathbf{S}_i \cdot \mathbf{S}_j - \sum_{i=1}^{N} D_i (S_i^z)^2 - H \sum_{i=1}^{N} S_i^z, \qquad (1.2)$$

where $\{D_i;\ i = 1, \ldots, N\}$ is a set of independent, quenched random variables, identically distributed according to a given probability density $P(D_i)$.

As we are mainly interested in the general features of the multicritical behavior, it is easier to look at the anisotropy-temperature phase diagram of the corresponding ferromagnetic models in zero field. Thus, we consider in this publication the ferromagnetic spin Hamiltonian

$$\mathcal{H} = -J \sum_{(i,j)} \mathbf{S}_i \cdot \mathbf{S}_j - \sum_{i=1}^{N} D_i (S_i^z)^2, \qquad (1.3)$$

with two types of double-delta distributions,

$$P_1(D_i) = p\,\delta(D_i - D) + (1-p)\,\delta(D_i), \qquad (1.4)$$

which describes a diluted anisotropy, and

$$P_2(D_i) = p\,\delta(D_i - D) + (1-p)\,\delta(D_i + D), \qquad (1.5)$$

which corresponds to a competition between anisotropies of opposite sign. We hope to gain some insight to consider the more relevant antiferromagnetic models in a future work.

We have also been motivated by many theoretical efforts to analyze a more complex class of models, given by the spin Hamiltonian

$$\mathcal{H} = -J \sum_{(i,j)} \mathbf{S}_i \cdot \mathbf{S}_j - D \sum_{i=1}^{N} (\hat{\mathbf{n}}_i \cdot \mathbf{S}_i)^2, \qquad (1.6)$$

where $\mathbf{S}_i$ is an m-component classical vector, and $\hat{\mathbf{n}}_i$ is a unit vector of random direction, which were introduced to describe amorphous rare earth transition-metal alloys[5]. For finite m, the mean-field phase diagram of the Random anisotropy axis model (RAM),

given by eq. (1.6), displays an ordered, ferromagnetic structure, and a disordered, paramagnetic structure[6]. In the m → ca limit, however, there is a pathological spin-glass phase. Momentum-space renormalization-group calculations in the spherical limit of infinite m yield an ordinary stable ferromagnetic fixed point that cannot be reached below four dimensions[7,8]. This lack of stability may be interpreted as a runaway of the flow lines, giving rise to a fluctuation-induced first-order transition. Some authors, however, give arguments to associate this instability with the occurrence of a spin-glass phase[9]. In the present publication, we use mean-field and momentum-space renormalization-group methods to analyze a simpler class of random models, given by the spin Hamiltonian (1.3), with a fixed axis of anisotropy. The mean-field phase diagrams, which can be obtained in full detail, do not display a spin-glass phase. Also, it is relatively easy to account for spin fluctuations through a momentum-space renormalization-group calculation in d dimensions, up to first order terms in the parameter $\epsilon = 4 - d$. As in the case of the random axis models, it seems difficult to reconcile the mean-field and the renormalization-group analyses.

The layout of this paper is as follows. Although it is known, in Section II we introduce the Curie–Weiss version of the pure model and analyze the main features of the phase diagram. The first-order boundary between ordered Ising and XY phases, at D = 0, ends at a stable bicritical point. In Section III, we present the mean-field results for the random models. Sections III.A to III.C refer to the probability distribution $P_1(D_i)$. For all values of p, there is only a bicritical point. Sections III.D to III.G refer to the probability distribution $P_2(D_i)$, with competing anisotropies. Besides the XY and Ising phases, there is also a Heisenberg phase in the ordered region of the mean-field phase diagram. Depending on p, the phase diagram may display more complex features, with a bicritical and a tetracritical point. In section IV, we present some preliminar~momentum-space renormalization-group calculations. In d dimensions, introducing n replicas of the original system, we obtain a set of recursion relations up to terms of order $\epsilon = 4 - d$. In the n → 0 limit, there is only a stable fixed point which cannot be reached from physically acceptable initial conditions. Higher-order calculations have to be performed to check the occurrence of fluctuation-induced first-order transitions. Some conclusions are presented in Section V.

II. Mean-field solution for the pure case

The long-range, Curie–Weiss, version of the Heisenberg ferromagnet in a uniaxial crystal field is given by the Hamiltonian

$$\mathcal{H} = -\frac{J}{2N}\sum_{i=1}^{N}\sum_{j=1}^{N}\mathbf{S}_i\cdot\mathbf{S}_i - D\sum_{i=1}^{N}(S_i^z)^2, \qquad (2.1)$$

where $J > 0$, and $\mathbf{S}_i$ is a three-dimensional classical vector of modulus S on the site i of a crystal lattice. The canonical partition function is written as

$$Z = \prod_{i=1}^{N}\left[\frac{1}{4\pi}\int_0^{2\pi}d\varphi_i\int_{-1}^{1}d(\cos\theta_i)\right]e^{-\beta\mathcal{H}}, \qquad (2.2)$$

where $\beta = (k_BT)^{-1}$, T is the absolute temperature, and the angle variables φ_i and θ_i are associated with the spin $\mathbf{S}_i$. Using the Gaussian identity

$$\sqrt{\pi}\,e^{a^2} = \int_{-\infty}^{\infty}dx\,e^{-x^2+2ax}, \qquad (2.3)$$

and performing the angle integrations, we have

$$Z = \left(\frac{N\beta JS^2}{2\pi}\right)^{3/2}\int d^3m\; e^{-N\beta g(\mathbf{m})}, \qquad (2.4)$$

where the mean-field Gibbs free-energy functional per site, in units of k_BT, is given by

$$\beta g = \frac{1}{2}(\tilde{m}_1^2+\tilde{m}_2^2)\,t - \ln\left[\int_0^1 d\xi\, e^{\tilde{d}\xi^2}\,I_0(\tilde{m}_1\sqrt{1-\xi^2})\cosh(\tilde{m}_2\xi)\right], \qquad (2.5)$$

where $t \equiv (\beta JS^2)^{-1}$, $d \equiv D/J$, $\tilde{d} \equiv d/t = \beta DS^2$, $\tilde{m}_1 \equiv m_1/t$, and $\tilde{m}_2 \equiv m_2/t$. The new variables $m_1 \equiv \sqrt{m_x^2 + m_y^2}$ and $m_2 \equiv m_z$ can be associated with the transverse and the longitudinal reduced magnetizations per site, and I_n is the n^{th}-order modified Bessel function of the first kind.

In the thermodynamic limit, $N \to \infty$, the Gibbs free energy per site can be obtained by the usual procedure of minimizing the mean-field Gibbs free-energy functional per site with respect to m_1 and m_2. The stationary conditions lead to the self-consistent equations of state,

$$m_1 = \tilde{m}_1 t = \frac{\int_0^1 d\xi\, e^{\tilde{d}\xi^2}\sqrt{1-\xi^2}\,I_1(\tilde{m}_1\sqrt{1-\xi^2})\cosh(\tilde{m}_2\xi)}{\int_0^1 d\xi\, e^{\tilde{d}\xi^2}\,I_0(\tilde{m}_1\sqrt{1-\xi^2})\cosh(\tilde{m}_2\xi)}, \qquad (2.6)$$

$$m_2 = \tilde{m}_2 t = \frac{\int_0^1 d\xi\, e^{\tilde{d}\xi^2}\,\xi\,I_0(\tilde{m}_1\sqrt{1-\xi^2})\sinh(\tilde{m}_2\xi)}{\int_0^1 d\xi\, e^{\tilde{d}\xi^2}\,I_0(\tilde{m}_1\sqrt{1-\xi^2})\cosh(\tilde{m}_2\xi)} \qquad (2.7)$$

Given the parameters of the model, if there are multiple solutions, we choose the values of m_1 and m_2 associated

with the absolute minimum of the Gibbs free-energy functional.

A. Analysis of the multicritical point

The critical behavior in the neighborhood of the paramagnetic lines comes from an expansion about the trivial paramagnetic saddle point solution, $m_1 = m_2 = 0$,

$$\beta g = -\ln A_0 + \frac{1}{2} r_1 \tilde{m}_1^2 + \frac{1}{2} r_2 \tilde{m}_2^2 + v_1 \tilde{m}_1^4 + 2v_{12} \tilde{m}_1^2 \tilde{m}_2^2 + v_2 \tilde{m}_2^4 + \mathcal{O}(\tilde{m}^6), \quad (2.8)$$

where the coefficients are given by

$$r_1 = t - \frac{1}{2}\left(1 - \frac{A_2}{A_0}\right), \quad (2.9)$$

$$r_2 = t - \frac{A_2}{A_0}, \quad (2.10)$$

$$v_1 = \frac{1}{64}\left[1 - 2\frac{A_2}{A_0} + 2\left(\frac{A_2}{A_0}\right)^2 - \frac{A_4}{A_0}\right], \quad (2.11)$$

$$v_{12} = \frac{1}{16}\left[\frac{A_4}{A_0} - \left(\frac{A_2}{A_0}\right)^2\right], \quad (2.12)$$

$$v_2 = \frac{1}{24}\left[3\left(\frac{A_2}{A_0}\right)^2 - \frac{A_4}{A_0}\right], \quad (2.13)$$

in terms of the integrals

$$A_n(\tilde{d}) \equiv \int_0^1 d\xi\, e^{\tilde{d}\xi^2} \xi^n. \quad (2.14)$$

The location of the paramagnetic second-order critical lines is given by $r_1 = 0$ and $r_2 = 0$, respectively. The multicritical point is given by $r_1 = r_2 = 0$. For r_1 and r_2 given by eqs. (2.9) and (2.10), the multicritical point is located at $t_c = \frac{1}{3}$ and $d_c = 0$. Although these results are exact for the long-range, Curie–Weiss version of the model, a Landau-type phenomenological analysis based on general symmetry arguments also leads to the same kind of expansion. A general mathematical stability analysis of the asymptotic solutions in the neighborhood of the multicritical point indicates two possibilities[10]. In one case, there are only two distinct ordered phase: near to the multicritical point. There is a pure perpendicularly ordered, or *XY-like* phase, with $m_1 \neq 0$ and $m_2 = 0$, and a pure parallel ordered or *Ising-like phase,* with $m_1 = 0$ and $m_2 \neq 0$. These pure phases are separated by a first-order transition line (a *flop* line), which ends at a *bicritical* point (where also meet the two second-order critical lines associated with the transitions from the paramagnetic phase). In the other case, the competition between the two types of ordering leads to the appearence of a third, intermediate, oblique, *Heisenberg-like* ordered phase, with $m_1 \neq 0$ and $m_2 \neq 0$. In this case, the first-order flop line splits into two second-order critical lines, separating the intermediate phase and each of the two pure ordered phases. The multicritical point at which all the four second-order critical lines meet together is then termed a tetracritical point.

The mathematical stability analysis of eq. (2.8) yields the following asymptotic solutions and corresponding free-energy densities :

- Paramagnetic solution $(\tilde{m}_1 = \tilde{m}_2 = 0)$

$$\beta g_P = -\ln A_0. \quad (2.15)$$

- XY-like solution $(\tilde{m}_1 \neq 0,\ \tilde{m}_2 = 0)$

$$\tilde{m}_1^2 \approx -\frac{r_1}{4v_1}, \quad (2.16)$$

$$\beta g_{XY} \approx -\ln A_0 - \frac{1}{16}\frac{r_1^2}{v_1}. \quad (2.17)$$

- Ising-like solution $(\tilde{m}_1 = 0,\ \tilde{m}_2 \neq 0)$

$$\tilde{m}_2^2 \approx -\frac{r_2}{4v_2}, \quad (2.18)$$

$$\beta g_I \approx -\ln A_0 - \frac{1}{16}\frac{r_2^2}{v_2}. \quad (2.19)$$

Heisenberg-like solution $(\tilde{m}_1 \neq 0,\ \tilde{m}_2 \neq 0)$

$$\tilde{m}_1^2 \approx \frac{r_1 v_2 - r_2 v_{12}}{4(v_{12}^2 - v_1 v_2)}, \quad (2.20)$$

$$\tilde{m}_2^2 \approx \frac{r_2 v_1 - r_1 v_{12}}{4(v_{12}^2 - v_1 v_2)}, \quad (2.21)$$

$$\beta g_H \approx \beta g_{XY} + \frac{(r_1 v_{12} - r_2 v_1)^2}{16 v_1 (v_{12}^2 - v_1 v_2)}, \quad (2.22)$$

$$= \beta g_I + \frac{(r_2 v_{12} - r_1 v_2)^2}{16 v_2 (v_{12}^2 - v_1 v_2)}. \quad (2.23)$$

To decide among these solutions, we have to look at the associated free energies. As the coefficients of the quartic terms, v_1 and v_2, are positive in the vicinity of the multicritical point, the sign of the difference $v_{12}^2 - v_1 v_2$ determines whether the point is bicritical (if $v_{12}^2 \geq v_1 v_2$) or tetracritical (if $v_{12}^2 < v_1 v_2$). Furthermore, the asymptotic solutions must vanish as we approach the multicritical point[10].

In the vicinity of the multicritical point we have

$$v_{12}^2 - v_1 v_2 = \frac{1}{1488375}\tilde{d}^2 + \mathcal{O}(\tilde{d}^3), \quad (2.24)$$

and

$$r_1 v_2 - r_2 v_{12} = -(r_2 v_1 - r_1 v_{12}) = \left(\frac{1}{150} - \frac{1}{35}|\tau|\right)\frac{1}{9}\tilde{d} + \mathcal{O}(\tilde{d}^2), \quad (2.25)$$

where

$$\tau = t - t_c = t - \frac{1}{3}. \quad (2.26)$$

Inserting these expansions into eqs. (2.20) and (2.21), we see that, in the particular case under consideration, the Heisenberg phase cannot exist in the neighborhood

of the multicritical point. Hence, the multicritical point of the pure system is of a bicritical nature.

B. Analysis of the ground state

The ground state can be obtained from the zero temperature limit of the equations of state and the free-energy density. We have the following possibilities.

- XY-like phase $(m_1 \neq 0,\ m_2 = 0)$

$$m_1 = \Theta\left(\frac{1}{2} - d\right), \tag{2.27}$$

$$\frac{1}{JS^2} g_{XY} = -\frac{1}{2}\Theta\left(\frac{1}{2} - d\right) - d\,\Theta\left(d - \frac{1}{2}\right), \tag{2.28}$$

where $\Theta(x)$ is the usual Heaviside step function,

$$\Theta(x) = \begin{cases} 0, & \text{for } x < 0, \\ 1, & \text{for } x > 0. \end{cases} \tag{2.29}$$

- Ising-like phase $(m_1 = 0,\ m_2 \neq 0)$

$$m_2 = \Theta\left(d + \frac{1}{2}\right), \tag{2.30}$$

$$\frac{1}{JS^2} g_I = -\left(d + \frac{1}{2}\right)\Theta\left(d + \frac{1}{2}\right) \tag{2.31}$$

As there are no solutions with $m_1 \neq 0$ and $m_2 \neq 0$, the Heisenberg phase does not exist even at zero temperature.

From eqs. (2.28) and (2.31) we have $g_{XY} > g_I$, for $d > 0$, and $g_{XY} < g_I$, for $d < 0$. Hence, the special point $d = t = 0$ belongs to a line of first-order transitions between the XY and Ising phases.

C. Global phase diagram

Along the $d = 0$ line, for $t < \frac{1}{3}$, the XY and Ising phases have the same free energies, as for an isotropic model. On the other hand, performing an expansion of the coefficients of the quartic terms about $\tilde{d} = 0$, and inserting them into the asymptotic expressions of the free-energy densities for the XY and Ising phases, given by eqs. (2.17) and (2.19), we obtain

$$\beta g_{XY} = -\ln A_0 - \frac{45}{4}r^2 - \tilde{d}\tau + \mathcal{O}(\tilde{d}\tau^2, \tilde{d}^2\tau), \tag{2.32}$$

$$\beta g_I = -\ln A_0 - \frac{45}{4}\tau^2 + 2\tilde{d}\tau + \mathcal{O}(\tilde{d}\tau^2, \tilde{d}^2\tau). \tag{2.33}$$

As $\tau < 0$ in the ordered region, for $d > 0$ the Ising phase has the lowest free energy, whereas, for $d < 0$, the XY phase is associated with the lowest free energy. Thus the line $d = 0$, for $t < t_c = \frac{1}{3}$, corresponds to a first-order boundary between the XY and Ising phases, whose magnetization densities are given by the non-trivial solutions of the integral equations

$$m_1 = \tilde{m}_1 t = \frac{\int_0^1 d\xi\, e^{\tilde{d}\xi^2}\sqrt{1-\xi^2}\, I_1(\tilde{m}_1\sqrt{1-\xi^2})}{\int_0^1 d\xi\, e^{\tilde{d}\xi^2} I_0(\tilde{m}_1\sqrt{1-\xi^2})},$$

$$\text{for } r_1 < 0 \text{ and } d < 0. \tag{2.34}$$

$$m_2 = \tilde{m}_2 t = \frac{\int_0^1 d\xi\, e^{\tilde{d}\xi^2}\,\xi \sinh(\tilde{m}_2\xi)}{\int_0^1 d\xi\, e^{\tilde{d}\xi^2}\cosh(\tilde{m}_2\xi)},$$

$$\text{for } r_2 < 0 \text{ and } d > 0. \tag{2.35}$$

From numerical and analytical (for $|\tilde{d}| \to \infty$) analyses, we see that $v_1 > \frac{1}{180}$, for $\frac{d}{t} < 0$, $v_2 > \frac{1}{180}$, for > 0, and $v_{12} > 0$, $\forall\ \frac{d}{t}$, and thus show that the second-order boundaries are completely stable, extending up to $|\tilde{d}| \to \infty$.

On the basis of the preceding results, we obtain the phase diagram of Fig. (1). As in the usual mean-field approxirnations, the second-order phase boundaries do not meet tangentially at the bicritical point.

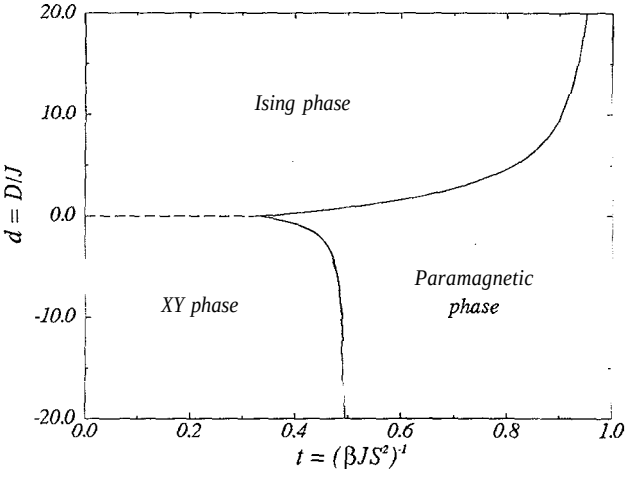

Figure 1: Mean-field phase diagram, in the anisotropy-ternperature plane, of the uniaxial Heisenberg ferromagnet. Solid lines represent second-order phase boundaries, whereas the dashed line represents a first-order boundary.

III. Mean-field solution for the random cases

The long-range, Curie–Weiss, version of the Heisenberg ferromagnet in a random uniaxial crystal field is given by the Hamiltonian

$$\mathcal{H} = -\frac{J}{2N}\sum_{i=1}^{N}\sum_{j=1}^{N}\mathbf{S}_i\cdot\mathbf{S}_j - \sum_{i=1}^{N} D_i\,(S_i^z)^2, \tag{3.1}$$

where J > 0, $\mathbf{S}_i$ is a three-dimensional classical vector of modulus S on the site i, and $\{D_i;\ i = 1, \ldots, N\}$ is a set of quenched, independent, identically distributed, random variables associated with a probability distribution $P(D_i)$.

As the calculations are very similar to the pure case, we give the main results only. The Gibbs free energy has to be averaged over the single-site random variables. For this self-averaging problem, we do not need to use the replica trick as in spin glasses.

In the thermodynamic limit, $N \to \infty$, by the strong law of large numbers, the mean-field Gibbs free-energy functional per site, in units of $k_B T$, is given by

$$\beta g = \frac{1}{2}(\tilde{m}_1^2 + \tilde{m}_2^2)\, t - \left\langle \ln \left[\int_0^1 d\xi\, e^{\tilde{d}_i \xi^2} I_0(\tilde{m}_1 \sqrt{1-\xi^2}) \cosh(\tilde{m}_2 \xi) \right] \right\rangle, \tag{3.2}$$

where we use the same notation as in the pure case (with $\tilde{d}_i = \beta D_i S^2$), and the averaging over the randomness is denoted by $\langle \cdots \rangle = \int dD_i \cdots P(D_i)$. From the stationary conditions, the transverse and the longitudinal reduced magnetizations per site, m_1 and m_2, satisfy the self-consistent equations of state,

$$m_1 = \tilde{m}_1 t = \left\langle \frac{\int_0^1 d\xi\, e^{\tilde{d}_i \xi^2} \sqrt{1-\xi^2}\, I_1(\tilde{m}_1 \sqrt{1-\xi^2}) \cosh(\tilde{m}_2 \xi)}{\int_0^1 d\xi\, e^{\tilde{d}_i \xi^2} I_0(\tilde{m}_1 \sqrt{1-\xi^2}) \cosh(\tilde{m}_2 \xi)} \right\rangle, \tag{3.3}$$

$$m_2 = \tilde{m}_2 t = \left\langle \frac{\int_0^1 d\xi\, e^{\tilde{d}_i \xi^2} \xi\, I_0(\tilde{m}_1 \sqrt{1-\xi^2}) \sinh(\tilde{m}_2 \xi)}{\int_0^1 d\xi\, e^{\tilde{d}_i \xi^2} I_0(\tilde{m}_1 \sqrt{1-\xi^2}) \cosh(\tilde{m}_2 \xi)} \right\rangle. \tag{3.4}$$

As in the pure case, we obtain a standard Landau expansion,

$$\beta g = -\left\langle \ln A_0(\tilde{d}_i) \right\rangle + \frac{1}{2}\left\langle r_1(\tilde{d}_i) \right\rangle \tilde{m}_1^2 + \frac{1}{2}\left\langle r_2(\tilde{d}_i) \right\rangle \tilde{m}_2^2 + \left\langle v_1(\tilde{d}_i) \right\rangle \tilde{m}_1^4 + 2\left\langle v_{12}(\tilde{d}_i) \right\rangle \tilde{m}_1^2 \tilde{m}_2^2 + \left\langle v_2(\tilde{d}_i) \right\rangle \tilde{m}_2^4 + \mathcal{O}(\tilde{m}^6), \tag{3.5}$$

where the coefficients, for a fixed configuration $\{D_i\}$ (before the averaging), are given by eqs. (2.9) to (2.14), replacing $\tilde{d}$ by $\tilde{d}_i$.

The analysis of Sections II.A–II.C can be repeated for the random case. In particular, let us consider two types of double-delta probability distributions,

$$P_1(D_i) = p\,\delta(D_i - D) + (1-p)\,\delta(D_i), \tag{3.6}$$

corresponding to a dilution of the anisotropy, and

$$P_2(D_i) = p\,\delta(D_i - D) + (1-p)\,\delta(D_i + D), \tag{3.7}$$

corresponding to a competition between two types of anisotropy.

For the probability distribution $P_1(D_i)$ there is only one multicritical point, as the paramagnetic second-order critical lines, defined by the conditions $\left\langle r_1(\tilde{d}_i) \right\rangle = 0$ and $\left\langle r_2(\tilde{d}_i) \right\rangle = 0$, intercept only once at the same multicritical point of the pure case. However, for the probability distribution $P_2(D_i)$, besides the multicritical point corresponding to the pure case, which is always present (except for the special case $p = \frac{1}{2}$), the phase diagram displays another multicritical point for $\frac{1}{3} < p < \frac{2}{3}$. As the main features of the phase diagram for the two cases are distinct, it is convenient to present separate analyses.

A. Analysis of the multicritical point for the probability distribution $P_1(D_i)$

In the vicinity of the multicritical point we have

$$\left\langle v_{12}(\tilde{d}_i) \right\rangle^2 - \left\langle v_1(\tilde{d}_i) \right\rangle \left\langle v_2(\tilde{d}_i) \right\rangle = \left(p - \frac{14}{15} \right) \left(\frac{1}{315} \right)^2 p\tilde{d}^2 + \mathcal{O}(\tilde{d}^3), \tag{3.8}$$

and

$$\left\langle r_1(\tilde{d}_i) \right\rangle \left\langle v_2(\tilde{d}_i) \right\rangle - \left\langle r_2(\tilde{d}_i) \right\rangle \left\langle v_{12}(\tilde{d}_i) \right\rangle = -\left[\left\langle r_2(\tilde{d}_i) \right\rangle \left\langle v_1(\tilde{d}_i) \right\rangle - \left\langle r_1(\tilde{d}_i) \right\rangle \left\langle v_{12}(\tilde{d}_i) \right\rangle \right] = \left(\frac{1}{150} - \frac{1}{35}|\tau| \right) \frac{p}{9}\tilde{d} + \mathcal{O}(\tilde{d}^2). \tag{3.9}$$

Inserting these expansions into the generalization of eqs. (2.20) and (2.21), we see that there is no possibility of existence of a Heisenberg phase in the neighborhood of the multicritical point. Hence, the multicritical point associated with this diluted distribution is always bicritical.

B. Analysis of the ground state for the probability distribution $P_1(D_i)$

As in the pure case, it is not difiicult to analyze the ground state for the probability distribution $P_1(D_i)$. Considering the zero temperature limit of the equations of state and the free-energy density, we have the following possibilities.

- *XY*-like phase ($m_1 \neq 0,\ m_2 = 0$)

$$m_1 = \Theta\left(\frac{1}{2} - d \right) + \left(\frac{1-p}{1-\frac{p}{2d}} \right) \Theta\left(d - \frac{1}{2} \right), \tag{3.10}$$

$$\frac{1}{JS^2}\, g_{XY} = -\frac{1}{2}\,\Theta\left(\frac{1}{2}-d\right) - \left[pd + \frac{1}{2}\frac{(1-p)^2}{1-\frac{p}{2d}}\right] \times \Theta\left(d-\frac{1}{2}\right). \quad (3.11)$$

• Ising-like phase ($m_1 = 0$, $m_2 \neq 0$)

$$m_2 = \left(\frac{1-p}{1+\frac{p}{2d}}\right)\Theta\left(-d-\frac{1}{2}\right) + \Theta\left(d+\frac{1}{2}\right), \quad (3.12)$$

$$\frac{1}{JS^2}\, g_I = -\frac{1}{2}\frac{(1-p)^2}{1+\frac{p}{2d}}\,\Theta\left(-d-\frac{1}{2}\right) - \left(pd+\frac{1}{2}\right) \times \Theta\left(d+\frac{1}{2}\right). \quad (3.13)$$

As there are no solutions with $m_1 \neq 0$ and $m_2 \neq 0$, the Heisenberg phase does not exist even at zero temperature.

From eqs. (3.11) and (3.13) we have $g_{XY} > g_I$, for d > 0, and $g_{XY} < g_I$, for d < 0. Hence, the special point d = t = 0 belongs to a line of first-order transitions between XY and Ising phases.

C. Global phase diagram for the probability distribution $P_1(D_i)$

Along the d = 0 line, for $t < \frac{1}{3}$, the XY and Ising phases have the same free energies, as for an isotropic model. On the other hand, performing an expansion of the coefficients of the quartic terms about $\tilde{d} = 0$, and inserting them into the asymptotic expressions of the free-energy densities for the XY and Ising phases, given by the generalization of eqs. (2.17) and (2.19), we obtain

$$\beta g_{XY} = -p \ln A_0(\tilde{d}) - \frac{45}{4}\tau^2 - p\tilde{d}\tau + \mathcal{O}(p\tilde{d}\tau^2, p\tilde{d}^2\tau), \quad (3.14)$$

$$\beta g_I = -p \ln A_0(\tilde{d}) - \frac{45}{4}\tau^2 + 2p\tilde{d}\tau + \mathcal{O}(p\tilde{d}\tau^2, p\tilde{d}^2\tau). \quad (3.15)$$

In analogy to the pure case, for d > 0 the Ising phase has the lowest free energy, whereas, for d < 0, the XY phase is associated with the lowest free energy. Thus, the dilution of the crystalline anisotropy does not alter the nature of the multicritical point, which remains bicritical. The line d = 0, for $t < t_c = \frac{1}{3}$, corresponds to a first-order boundary between the XY and Ising phases, whose magnetization densities are given by the non-trivial solutions of the integral equations

$$m_1 = \tilde{m}_1 t = p\,\frac{\int_0^1 d\xi\, e^{\tilde{d}\xi^2}\sqrt{1-\xi^2}\, I_1(\tilde{m}_1\sqrt{1-\xi^2})}{\int_0^1 d\xi\, e^{\tilde{d}\xi^2} I_0(\tilde{m}_1\sqrt{1-\xi^2})} + (1-p)\,\mathcal{L}(\tilde{m}_1), \text{ for } \left\langle r_1(\tilde{d}_i)\right\rangle < 0 \text{ and } d < 0, \quad (3.16)$$

$$m_2 = \tilde{m}_2 t = p\,\frac{\int_0^1 d\xi\, e^{\tilde{d}\xi^2}\,\xi\sinh(\tilde{m}_2\xi)}{\int_0^1 d\xi\, e^{\tilde{d}\xi^2}\cosh(\tilde{m}_2\xi)} + (1-p)\,\mathcal{L}(\tilde{m}_2), \text{ for } \left\langle r_2(\tilde{d}_i)\right\rangle < 0 \text{ and } d > 0, \quad (3.17)$$

where

$$\mathcal{L}(x) \equiv \coth x - \frac{1}{x} \quad (3.18)$$

is the Langevin function.

The phase diagram is topologically similar to the pure case. The only difference is the retraction of the asymptotes of the second-order phase boundaries, which get closer to the bicritical temperature as the value of the distribution parameter p is reduced. Varying this parameter, the asymptotic temperatures of the second-order boundaries between the paramagnetic and the Ising and XY phases are respectively shifted to

$$t_+ = \frac{1}{3}(1+2p), \quad \text{for } d \to +\infty, \quad (3.19)$$

and

$$t_- = \frac{1}{3}\left(1+\frac{p}{2}\right), \quad \text{for } d \to -\infty. \quad (3.20)$$

The stabiiity analysis also indicates that the lines of second-order transitions are completely stable, extending up to $|\tilde{d}| \to \infty$.

D. Analyses of the multicritical points for the probability distribution $P_2(D_i)$

For the probability distribution $P_2(D_i)$, besides the trivial multicritical point located at $t_c^{(1)} = \frac{1}{3}$ and $d_c^{(1)} = 0$, the phase diagrams can display, for $\frac{1}{3} < p < \frac{2}{3}$ (except for $p = \frac{1}{2}$), another multicritical point, located at $t_c^{(2)} = \frac{1}{3}$ and $d_c^{(2)} \neq 0$.

D.1. Analysis of the trivial multicritical point, $t_c^{(1)} = \frac{1}{3}$ and $d_c^{(1)} = 0$

In the vicinity of the trivial multicritical point we have

$$\left\langle v_{12}(\tilde{d}_i)\right\rangle^2 - \left\langle v_1(\tilde{d}_i)\right\rangle\left\langle v_2(\tilde{d}_i)\right\rangle = \left[(1-2p)^2 - \frac{14}{15}\right]\left(\frac{1}{315}\right)^2\tilde{d}^2 + \mathcal{O}(\tilde{d}^3), \quad (3.21)$$

and

$$\left\langle r_1(\tilde{d}_i)\right\rangle\left\langle v_2(\tilde{d}_i)\right\rangle - \left\langle r_2(\tilde{d}_i)\right\rangle\left\langle v_{12}(\tilde{d}_i)\right\rangle = -\left[\left\langle r_2(\tilde{d}_i)\right\rangle\left\langle v_1(\tilde{d}_i)\right\rangle - \left\langle r_1(\tilde{d}_i)\right\rangle\left\langle v_{12}(\tilde{d}_i)\right\rangle\right] = \left(\frac{1}{150} - \frac{1}{35}|\tau|\right)(2p-1)\frac{\tilde{d}}{9} + \mathcal{O}(\tilde{d}^2). \quad (3.22)$$

Inserting these expansions into the generalization of

eqs. (2.20) and (2.21), we see that there is no possibility of existence of a Heisenberg phase in the neighborhood of the trivial multicritical point. For the special case $p = \frac{1}{2}$, we obtain

$$\tilde{m}_1^2 \approx -\frac{315}{8}\left(\frac{1}{21} - |\tau|\right), \tag{3.23}$$

$$\tilde{m}_2^2 \approx \frac{45}{8}\left(\frac{1}{3} + |\tau|\right), \tag{3.24}$$

contradicting our initial assumption that m_1 and m_2 vanish at the multicritical point. Hence, the trivial multicritical point is always bicritical.

D.2. Analysis of the non-trivial multicritical point, $t_c^{(2)} = \frac{1}{3}$ and $d_c^{(2)} \neq 0$

For $\frac{1}{3} < p < \frac{2}{3}$ (except for the special case $p = \frac{1}{2}$), the paramagnetic second-order critical lines, defined by the conditions $\left\langle r_1(\tilde{d}_i)\right\rangle = 0$ and $\left\langle r_2(\tilde{d}_i)\right\rangle = 0$, intercept more than once. Besides the trivial multicritical point, there is a non-trivial multicritical point, located at $t_c^{(2)} = \frac{1}{3}$ and $d_c^{(2)} \neq 0$, whose coordinate $d_c^{(2)}$ is given by the solution of the equation

$$p = \frac{\frac{1}{3} - \frac{A_2(-3d_c^{(2)})}{A_0(-3d_c^{(2)})}}{\frac{A_2(3d_c^{(2)})}{A_0(3d_c^{(2)})} - \frac{A_2(-3d_c^{(2)})}{A_0(-3d_c^{(2)})}}. \tag{3.25}$$

As $d_c^{(2)}$ cannot be obtained in closed form, we must rely on numerical results. In particular, we can verify that the solution $d_c^{(2)}$, for a given value of p, always satisfies the tetracriticality eondition, $\left\langle v_{12}(\tilde{d}_i)\right\rangle^2 - \left\langle v_1(\tilde{d}_i)\right\rangle\left\langle v_2(\tilde{d}_i)\right\rangle < 0$. Hence, whenever it exists, the non-trivial multicritical point is always tetracritical.

E. Analysis of the ground state for the probability distribution $P_2(D_i)$

As in the pure case, it is not difficult to analyze the ground state for the probability distribution $P_2(D_i)$. Considering the zero temperature limit of the equations of state and the free-energy density, we have the following possibilities.

• XY-like phase ($m_1 \neq 0$, $m_2 = 0$)

$$m_1 = \left(\frac{p}{1+\frac{1-p}{2d}}\right)\Theta\left(-d-\frac{1}{2}\right) + \Theta\left(d+\frac{1}{2}\right)\Theta\left(\frac{1}{2}-d\right) + \left(\frac{1-p}{1-\frac{p}{2d}}\right)\Theta\left(d-\frac{1}{2}\right), \tag{3.26}$$

$$\frac{1}{JS^2}g_{XY} = \left[(1-p)d - \frac{1}{2}\frac{p^2}{1+\frac{1-p}{2d}}\right]\Theta\left(-d-\frac{1}{2}\right) - \frac{1}{2}\Theta\left(d+\frac{1}{2}\right)\Theta\left(\frac{1}{2}-d\right) - \left[pd + \frac{1}{2}\frac{(1-p)^2}{1-\frac{p}{2d}}\right]\Theta\left(d-\frac{1}{2}\right). \tag{3.27}$$

• Ising-like phase ($m_1 = 0$, $m_2 \neq 0$)

$$m_2 = \left(\frac{1-p}{1+\frac{p}{2d}}\right)\Theta\left(-d-\frac{1}{2}\right) + \Theta\left(d+\frac{1}{2}\right)\Theta\left(\frac{1}{2}-d\right) + \left(\frac{p}{1-\frac{1-p}{2d}}\right)\Theta\left(d-\frac{1}{2}\right), \tag{3.28}$$

$$\frac{1}{JS^2}g_I = \left[(1-p)d - \frac{1}{2}\frac{(1-p)^2}{1+\frac{p}{2d}}\right]\Theta\left(-d-\frac{1}{2}\right) - \left[\frac{1}{2} - (1-2p)d\right]\Theta\left(d+\frac{1}{2}\right)\Theta\left(\frac{1}{2}-d\right) - \left[pd + \frac{1}{2}\frac{p^2}{1-\frac{1-p}{2d}}\right]\Theta\left(d-\frac{1}{2}\right). \tag{3.29}$$

• Heisenberg-like phase ($m_1 \neq 0$, $m_2 \neq 0$)

$$m_1 = p\cos\phi + (1-p)\cos\psi, \tag{3.30}$$

$$m_2 = p\sin\phi + (1-p)\sin\psi, \tag{3.31}$$

where the angles ϕ and ψ are defined by the relations

$$\cos\phi = -\frac{d}{p}\cos\psi\left[1 - \mathrm{sgn}(d)\sqrt{1+\frac{p(1-p)}{d^2}}\right], \tag{3.32}$$

$$\sin\phi = \frac{d}{p}\sin\psi\left[1 + \mathrm{sgn}(d)\sqrt{1+\frac{p(1-p)}{d^2}}\right], \tag{3.33}$$

$$\cos\psi = \frac{1}{\sqrt{2}}\sqrt{1 + \mathrm{sgn}(d)\frac{1+\frac{p(1-2p)}{2d^2}}{\sqrt{1+\frac{p(1-p)}{d^2}}}}, \tag{3.34}$$

$$\sin\psi = \frac{1}{\sqrt{2}}\sqrt{1 - \mathrm{sgn}(d)\frac{1+\frac{p(1-2p)}{2d^2}}{\sqrt{1+\frac{p(1-p)}{d^2}}}}, \tag{3.35}$$

$$\frac{1}{JS^2}g_H = -\frac{1}{2} + p(1-p) + \frac{1}{2}(1-2p)d - \frac{|d|}{2}\sqrt{1+\frac{p(1-p)}{d^2}}. \tag{3.36}$$

From the expressions for the free-energy densities, it follows that, whenever the Heisenberg phase exists, for

$$|d| > \frac{1}{2}|2p-1|, \tag{3.37}$$

the associated free energy is lower than for the XY and the Ising phases. On the other hand, the free energies for the XY and Ising phases satisfy the relations

$$g_{XY} > g_I, \quad \text{for } (1-2p)d < 0 \text{ and } d \in [-\tfrac{1}{2}, \tfrac{1}{2}], \tag{3.38}$$

$$g_{XY} < g_I, \quad \text{for } (1-2p)d > 0 \text{ and } d \in [-\tfrac{1}{2}, \tfrac{1}{2}]. \tag{3.39}$$

Hence, the special point $d = t = 0$ belongs to a line of first-order transitions between the XY and Ising phases, and the points $d = \pm\frac{1}{2}|2p-1|$, $t = 0$, belong to lines of second-order transitions between the Heisenberg and the XY and the Ising phases.

F. Analysis of the second-order boundaries in the ordered region for the probability distribution $P_2(D_i)$

As the analyses of the non-trivial multicritical point and the ground state reveal the existence of a Heisenberg phase, we should find the lines of second-order transitions between this phase and the XY and the Ising phases. These second-order boundaries can be obtained from the expansion of the free-energy density in terms of the critical magnetization density,

$$\beta g = \beta g_\perp + \frac{1}{2}\left\langle r_\perp(\tilde{d}_i)\right\rangle \tilde{m}_2^2 + \left\langle v_\perp(\tilde{d}_i)\right\rangle \tilde{m}_2^4 + \mathcal{O}(\tilde{m}_2^6) \tag{3.40}$$

$$= \beta g_\parallel + \frac{1}{2}\left\langle r_\parallel(\tilde{d}_i)\right\rangle \tilde{m}_1^2 + \left\langle v_\parallel(\tilde{d}_i)\right\rangle \tilde{m}_1^4 + \mathcal{O}(\tilde{m}_1^6), \tag{3.41}$$

where the regular parts of the free-energy density are given by

$$\beta g_\perp = \frac{1}{2}\tilde{m}_1^2 t - \left\langle \ln\left[\int_0^1 d\xi\, e^{\tilde{d}_i\xi^2} I_0(\tilde{m}_1\sqrt{1-\xi^2})\right]\right\rangle, \tag{3.42}$$

$$\beta g_\parallel = \frac{1}{2}\tilde{m}_2^2 t - \left\langle \ln\left[\int_0^1 d\xi\, e^{\tilde{d}_i\xi^2} \cosh(\tilde{m}_2\xi)\right]\right\rangle, \tag{3.43}$$

and the coefficients of the expansion, for a fixed configuration $\{D_i\}$ (before the averaging), are given by

$$r_\perp(\tilde{d}_i) = t - \frac{\displaystyle\int_0^1 d\xi\, e^{\tilde{d}_i\xi^2}\xi^2 I_0(\tilde{m}_1\sqrt{1-\xi^2})}{\displaystyle\int_0^1 d\xi\, e^{\tilde{d}_i\xi^2} I_0(\tilde{m}_1\sqrt{1-\xi^2})}, \tag{3.44}$$

$$r_\parallel(\tilde{d}_i) = t - \frac{1}{2}\frac{\displaystyle\int_0^1 d\xi\, e^{\tilde{d}_i\xi^2}(1-\xi^2)\cosh(\tilde{m}_2\xi)}{\displaystyle\int_0^1 d\xi\, e^{\tilde{d}_i\xi^2}\cosh(\tilde{m}_2\xi)}, \tag{3.45}$$

$$v_\perp(\tilde{d}_i) = \frac{1}{8}\left[\frac{\displaystyle\int_0^1 d\xi\, e^{\tilde{d}_i\xi^2}\xi^2 I_0(\tilde{m}_1\sqrt{1-\xi^2})}{\displaystyle\int_0^1 d\xi\, e^{\tilde{d}_i\xi^2} I_0(\tilde{m}_1\sqrt{1-\xi^2})}\right]^2 - \frac{1}{24}\frac{\displaystyle\int_0^1 d\xi\, e^{\tilde{d}_i\xi^2}\xi^4 I_0(\tilde{m}_1\sqrt{1-\xi^2})}{\displaystyle\int_0^1 d\xi\, e^{\tilde{d}_i\xi^2} I_0(\tilde{m}_1\sqrt{1-\xi^2})}, \tag{3.46}$$

$$v_\parallel(\tilde{d}_i) = \frac{1}{32}\left[\frac{\displaystyle\int_0^1 d\xi\, e^{\tilde{d}_i\xi^2}(1-\xi^2)\cosh(\tilde{m}_2\xi)}{\displaystyle\int_0^1 d\xi\, e^{\tilde{d}_i\xi^2}\cosh(\tilde{m}_2\xi)}\right]^2 - \frac{1}{64}\frac{\displaystyle\int_0^1 d\xi\, e^{\tilde{d}_i\xi^2}(1-\xi^2)^2\cosh(\tilde{m}_2\xi)}{\displaystyle\int_0^1 d\xi\, e^{\tilde{d}_i\xi^2}\cosh(\tilde{m}_2\xi)}. \tag{3.47}$$

Notice that these coefficients depend on the non-critical magnetization densities, which come from the stationary conditions, $\partial g_\perp/\partial\tilde{m}_1 = 0$ and $\partial g_\parallel/\partial\tilde{m}_2 = 0$, respectively.

Hence, the line of second-order transitions between the Heisenberg and XY phases is given by $\left\langle r_\perp(\tilde{d}_i)\right\rangle = 0$, supplemented by the stability condition, $\left\langle v_\perp(\tilde{d}_i)\right\rangle > 0$, while the lines of second-order transitions between the Heisenberg and Ising phases are given by $\left\langle r_\parallel(\tilde{d}_i)\right\rangle = 0$, supplemented by the stability condition, $\left\langle v_\parallel(\tilde{d}_i)\right\rangle > 0$. We have performed numerical calculations to locate these lines and to check the validity of the stability requirements.

G. Global phase diagram for the probability distribution $P_2(D_i)$

Along the $d = 0$ line, for $t < \frac{1}{3}$, the XY and Ising phases have the same free energies, as for an isotropic model. On the other hand, performing an expansion of the coefficients of the quartic terms about $d = 0$, and

inserting them into the asymptotic expressions of the free-energy densities for the XY and Ising phases, given by the generalization of eqs. (2.17) and (2.19), we obtain

$$\beta g_{XY} = -\,p\ln A_0(\tilde{d}) - (1-p)\ln A_0(-\tilde{d}) - \frac{45}{4}\tau^2 - (2p-1)\,\tilde{d}\tau + \mathcal{O}(p\tilde{d}\tau^2, p\tilde{d}^2\tau), \tag{3.48}$$

$$\beta g_I = -\,p\ln A_0(\tilde{d}) - (1-p)\ln A_0(-\tilde{d}) - \frac{45}{4}\tau^2 + 2(2p-1)\,\tilde{d}\tau + \mathcal{O}(p\tilde{d}\tau^2, p\tilde{d}^2\tau). \tag{3.49}$$

Thus, for $(1-2p)\tilde{d} < 0$, the Ising phase has the lowest free energy, whereas, for $(1-2p)\tilde{d} > 0$, the XY phase is associated with the lowest free energy. Thus, the competitive and symmetric distribution $P_2(D_i)$ does not alter the nature of the trivial multicritical point, which remains bicritical.

For p = $\frac{1}{2}$, we have to keep the expansions of the coefficients up to terms of second order in $\tilde{d}$,

$$\beta g_{XY} = -\,\frac{1}{2}\left[\ln A_0(\tilde{d}) + \ln A_0(-\tilde{d})\right] - \frac{45}{4}\tau^2 - \frac{2}{21}\tilde{d}^2\tau + \mathcal{O}(\tilde{d}^2\tau^2), \tag{3.50}$$

$$\beta g_I = -\,\frac{1}{2}\left[\ln A_0(\tilde{d}) + \ln A_0(-\tilde{d})\right] - \frac{45}{4}\tau^2 + \frac{4}{21}\tilde{d}^2\tau + \mathcal{O}(\tilde{d}^2\tau^2). \tag{3.51}$$

In the special case p = $\frac{1}{2}$, the transitions, and hence the multicritical points, disappear, as the Ising phase has always a lower free energy.

For p # $\frac{1}{2}$, the line d = 0, for $t < t_c = \frac{1}{3}$, corresponds to a first-order boundary between the XY and Ising phases, whose magnetization densities are given by the non-trivial solutions of the integral equations

$$m_1 = p\,\frac{\int_0^1 d\xi\, e^{\tilde{d}\xi^2}\sqrt{1-\xi^2}\,I_1(\tilde{m}_1\sqrt{1-\xi^2})}{\int_0^1 d\xi\, e^{\tilde{d}\xi^2} I_0(\tilde{m}_1\sqrt{1-\xi^2})} + (1-p)\,\frac{\int_0^1 d\xi\, e^{-\tilde{d}\xi^2}\sqrt{1-\xi^2}\,I_1(\tilde{m}_1\sqrt{1-\xi^2})}{\int_0^1 d\xi\, e^{-\tilde{d}\xi^2} I_0(\tilde{m}_1\sqrt{1-\xi^2})},$$

for $\left\langle r_1(\tilde{d}_i)\right\rangle < 0$, and (1 – 2p)d > 0, with $\left\langle r_\perp(\tilde{d}_i)\right\rangle > 0$, and (3.52)

$$m_2 = p\,\frac{\int_0^1 d\xi\, e^{\tilde{d}\xi^2}\,\xi\,\sinh(\tilde{m}_2\xi)}{\int_0^1 d\xi\, e^{\tilde{d}\xi^2}\cosh(\tilde{m}_2\xi)} + (1-p)\,\frac{\int_0^1 d\xi\, e^{-\tilde{d}\xi^2}\,\xi\,\sinh(\tilde{m}_2\xi)}{\int_0^1 d\xi\, e^{-\tilde{d}\xi^2}\cosh(\tilde{m}_2\xi)},$$

for $\left\langle r_2(\tilde{d}_i)\right\rangle < 0$, and (1 – 2p)d < 0, with $\left\langle r_\parallel(\tilde{d}_i)\right\rangle > 0$. (3.53)

Second-order boundaries separate these two phases from the Heisenberg phase, whose magnetization densities are given by the simultaneous non-trivial solutions of the integral equations (3.3) and (3.4). These solutions exist when the conditions $\left\langle r_\perp(\tilde{d}_i)\right\rangle > 0$ or $\left\langle r_\parallel(4))\right\rangle > 0$ are not satisfied for the XY and the Ising phases, respectively.

On the basis of the preceding results, we obtain the phase diagrams shown in Figs. (2) to (4). Due to the invariance by the changes p → (1 – p), d → $-d$, it is sufficient to obtain the phase diagrams for $\frac{1}{2} \le$ p < 1.

IV. Renormalization-group treatment

Despite the richness of the mean-field phase diagrams, it is important to investigate whether these mean-field results remain unchanged if we consider a realistic model with short-range interactions. To account for the spin fluctuations, let us perform a renormalization-group calculation for the short-range version of the model. In this case, the canonical partition function, for a fixed configuration $\{D_i\}$, is given by

$$Z_D = \prod_{i=1}^{N}\left[\frac{1}{4\pi}\int_0^{2\pi} d\varphi_i \int_{-1}^{1} d(\cos\theta_i)\right] e^{-\beta\mathcal{H}(\{D_i\})}, \tag{4.1}$$

with

$$-\beta\mathcal{H}\left(\{D_i\}\right) = \frac{1}{2}\sum_{i,j} K_{ij}\,\mathbf{S}_i\cdot\mathbf{S}_j + \sum_{i=1}^{N}\beta D_i\,(S_i^z)^2, \tag{4.2}$$

where i, j are sites on a d-dimensional hypercubic lattice, $\mathbb{K}$ is an N×N matrix with elements $K_{ij} = \beta J > 0$, if i and j are nearest neighbors, and $K_{ij} = 0$, otherwise, and the angle variables φ_i and θ_i are associated with the vector $\mathbf{S}_i$.

Using the generalized Gaussian transformation,

$$\exp\left[\frac{1}{2}\sum_{i,j} K_{ij}\,\mathbf{S}_i\cdot\mathbf{S}_j\right] = [\det\mathbb{K}]^{-3/2}\left[\prod_{i=1}^{N}\int\frac{d^3\sigma_i}{\pi^{3/2}}\right] \times \exp\left[-\frac{1}{2}\sum_{i,j}(K^{-1})_{ij}\,\sigma_i\cdot\sigma_j + \sum_{i=1}^{N}\mathbf{S}_i\cdot\sigma_i\right], \tag{4.3}$$

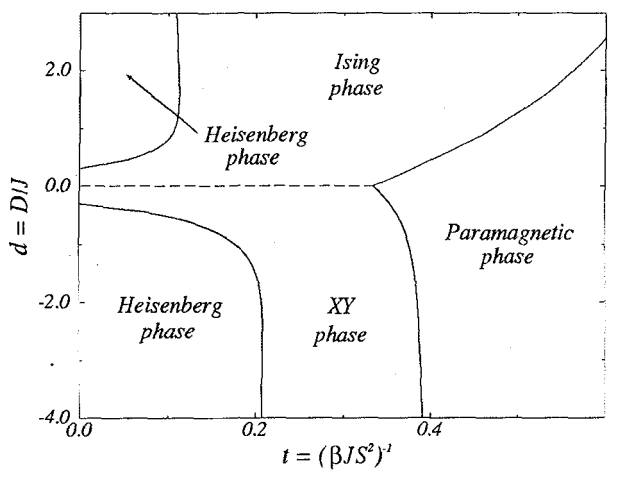

Figure 2: Typical mean-field phase diagram for $\frac{2}{3} \leq p < 1$ (this figure was drawn for $p = 0.8$), in the anisotropy-temperature plane, of the random uniaxial Heisenberg ferromagnet for the probability distribution $P_2(D_i)$. Solid lines represent second-order phase boundaries, whereas the dashed line represents a first-order boundary. A Heisenberg phase is always present at lower temperatures and stronger anisotropies.

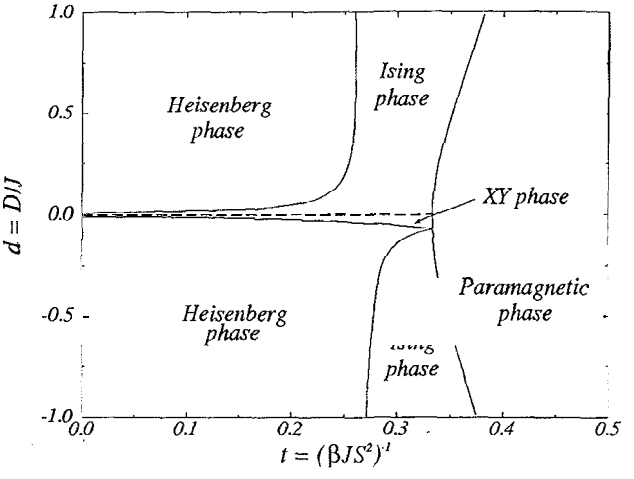

Figure 3: Typical mean-field phase diagram for $\frac{1}{2} < p < \frac{2}{3}$ (this figure was drawn for $p = 0.51$), in the anisotropy-temperature plane, of the random uniaxial Heisenberg ferromagnet for the probability distribution $P_2(D_i)$. Solid lines represent second-order phase boundaries, whereas the dashed line represents a first-order boundary. Notice that, besides the trivial bicritical point, there is also a tetracritical point.

we introduce a new three-dimensional spin field. Integrating over the angle variables, introducing n replicas and averaging over the randomness, we have

$$\langle Z_D^n \rangle = [\det \mathbb{K}]^{-3n/2} \left[\prod_{\alpha=1}^{n} \prod_{i=1}^{N} \int \frac{d^3\sigma_i^\alpha}{\pi^{3/2} S^3} \right] \exp \left[-\frac{1}{2} \sum_{\alpha=1}^{n} \sum_{i,j} \frac{1}{S^2} (K^{-1})_{ij}\, \sigma_i^\alpha \cdot \sigma_j^\alpha \right.$$
$$\left. + \sum_{i=1}^{N} \ln \left\langle \prod_{\alpha=1}^{n} \int_0^1 d\xi_i\, e^{\tilde{d}_i \xi_i^2}\, I_0(\sigma_{1i}^\alpha \sqrt{1-\xi_i^2})\, \cosh(\sigma_{2i}^\alpha \xi_i) \right\rangle \right], \qquad (4.4)$$

where the index $\alpha = 1, \ldots, n$ labels distinct replicas.

The suitable effective Hamiltonian to perform the renormalization-group calculations can be obtained according to the following steps : (i) an expansion of the integrand of $\langle Z_D^n \rangle$ about the paramagnetic solution up to fourth-order terms in the new spin fields, $\sigma_1 \equiv (\sigma_x, \sigma_y)$ and $\sigma_2 \equiv \sigma_z$; (ii) a d-dimensional Fourier transformation, $\hat{\sigma}(\mathbf{q}) = \sum_{\mathbf{r}} \sigma(\mathbf{r}) e^{i\mathbf{q}\cdot\mathbf{r}}$; (iii) a low-momentum expansion of the quadratic coefficients using the ferromagnetic nearest-neighbor interactions; (iv) a rescaling of the momentum-space spin fields to normalize the coefficients of the $\mathbf{q}^2$ terms.

Thus, in the continuum limit, the reduced effective Landau–Ginzburg–Wilson Hamiltonian in momentum-space, $\bar{\mathcal{H}}_{\rm ef} = -\beta \mathcal{H}_{\rm ef} = \bar{\mathcal{H}}_0 + \bar{\mathcal{H}}_p$, is separated into a Gaussian term,

$$\bar{\mathcal{H}}_0 = -\frac{1}{2} \sum_{\alpha} \int_{\mathbf{q}_1} \int_{\mathbf{q}_2} \left[(r_1 + \mathbf{q}_1^2)\, \hat{\sigma}_1^\alpha(\mathbf{q}_1) \cdot \hat{\sigma}_1^\alpha(\mathbf{q}_2) + (r_2 + \mathbf{q}_2^2)\, \hat{\sigma}_2^\alpha(\mathbf{q}_1) \hat{\sigma}_2^\alpha(\mathbf{q}_2) \right] \delta(\mathbf{q}_1 + \mathbf{q}_2), \qquad (4.5)$$

and a quartic perturbation,

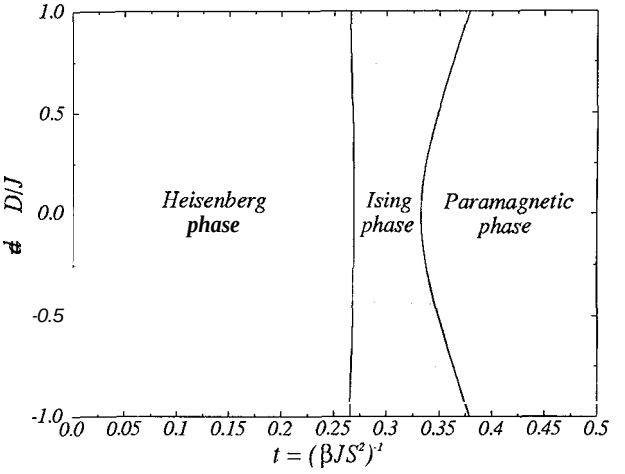

Figure 4: Mean-field phase diagram for the special case p = $\frac{1}{2}$, in the anisotropy-temperature plane, of the random uniaxial Heisenberg ferromagnet for the probability distribution $P_2(D_i)$. The solid lines represent second-order phase boundaries. The XY phase is no longer present and the trivial bicritical and tetracritical points tlisappear.

$$\begin{aligned}
\bar{\mathcal{H}}_p = &- \sum_{\alpha,\beta} (u_1 + v_1\,\delta_{\alpha\beta}) \int_{\mathbf{q}_1}\int_{\mathbf{q}_2}\int_{\mathbf{q}_3}\int_{\mathbf{q}_4} \hat{\sigma}_1^{\alpha}(\mathbf{q}_1)\cdot\hat{\sigma}_1^{\alpha}(\mathbf{q}_2)\,\hat{\sigma}_1^{\beta}(\mathbf{q}_3)\cdot\hat{\sigma}_1^{\beta}(\mathbf{q}_4)\,\delta(\mathbf{q}_1+\mathbf{q}_2+\mathbf{q}_3+\mathbf{q}_4) \\
&- 2\sum_{\alpha,\beta} (u_{12} + v_{12}\,\delta_{\alpha\beta}) \int_{\mathbf{q}_1}\int_{\mathbf{q}_2}\int_{\mathbf{q}_3}\int_{\mathbf{q}_4} \hat{\sigma}_1^{\alpha}(\mathbf{q}_1)\cdot\hat{\sigma}_1^{\alpha}(\mathbf{q}_2)\,\hat{\sigma}_2^{\beta}(\mathbf{q}_3)\hat{\sigma}_2^{\beta}(\mathbf{q}_4)\,\delta(\mathbf{q}_1+\mathbf{q}_2+\mathbf{q}_3+\mathbf{q}_4) \\
&- \sum_{\alpha,\beta} (u_2 + v_2\,\delta_{\alpha\beta}) \int_{\mathbf{q}_1}\int_{\mathbf{q}_2}\int_{\mathbf{q}_3}\int_{\mathbf{q}_4} \hat{\sigma}_2^{\alpha}(\mathbf{q}_1)\hat{\sigma}_2^{\alpha}(\mathbf{q}_2)\hat{\sigma}_2^{\beta}(\mathbf{q}_3)\hat{\sigma}_2^{\beta}(\mathbf{q}_4)\,\delta(\mathbf{q}_1+\mathbf{q}_2+\mathbf{q}_3+\mathbf{q}_4), \qquad (4.6)
\end{aligned}$$

where $\int_{\mathbf{q}} \equiv \left(\frac{1}{2\pi}\right)^d \int d^d q$ denotes integration over the first Brillouin zone of a d-dimensional hypercubic lattice and the cosfficients can be expressed in terms of the original paiameters of the model.

According to the standard renormalization-group procedures, we choose a rescaling factor $b > 1$ and perform a functional integration over spin variables such that $1/b < |\mathbf{q}|a/\pi < 1$, where a is the lattice spacing. Ignoring irrelevant terms, we rescale the momenta $\mathbf{q}$ and the remaining spin variables, so that the renormalized Hamiltonian can be written in the same form as in eqs. *(4.5)*and (4.6), but with new parameters. To first order in $\epsilon = 4 - d$, the renormalization-group recursion relations are given by

$$r_1' = b^2\left\{ r_1 + 4A\Big[2(n+1)u_1 + 4v_1 + nu_{12} + v_{12}\Big]\right\}, \qquad (4.7)$$

$$r_2' = b^2\left\{ r_2 + 4A\Big[(n+2)u_2 + 3v_2 + 2(nu_{12} + v_{12})\Big]\right\}, \qquad (4.8)$$

$$u_1' = b^{\epsilon}\left\{ u_1 - 4u_1K_4\ln b\Big[2(n+4)u_1 + 8v_1\Big] - 4u_{12}K_4\ln b\,(nu_{12} + 2v_{12})\right\}, \qquad (4.9)$$

$$u_{12}' = b^{\epsilon}\left\{ u_{12} - 4u_{12}K_4\ln b\Big[2(n+1)u_1 + (n+2)u_2 + 4v_1 + 3v_2 + 4u_{12}\Big] - 4v_{12}K_4\ln b\,(2u_1 + u_2)\right\}, \qquad (4.10)$$

$$u_2' = b^{\epsilon}\left\{ u_2 - 4u_2K_4\ln b\Big[(n+8)u_2 + 6v_2\Big] - 8u_{12}K_4\ln b\,(nu_{12} + 2v_{12})\right\}, \qquad (4.11)$$

$$v_1' = b^{\epsilon}\left\{ v_1 - 8v_1K_4\ln b\,(6u_1 + 5v_1) - 4v_{12}^2K_4\ln b\right\}, \qquad (4.12)$$

$$v_{12}' = b^{\epsilon}\,v_{12}\left\{ 1 - 4K_4\ln b\Big[2(u_1 + u_2) + 4v_1 + 3v_2 + 4v_{12} + 8u_{12}\Big]\right\}, \qquad (4.13)$$

$$v_2' = b^{\epsilon}\left\{ v_2 - 12v_2K_4\ln b\,(4u_2 + 3v_2) - 8v_{12}^2K_4\ln b\right\}, \qquad (4.14)$$

where $A = \frac{1}{2}K_4(1 - b^{-2})\left(\frac{\pi}{a}\right)^2$ and $K_d^{-1} = 2^{d-1}\pi^{d/2}\,\Gamma\left(\frac{1}{2}d\right)$.

In the pure case, for which $u_1 = u_{12} = u_2 = 0$, we recover the results obtained by Kosterlitz et al.[11] in the study of multicritical points in anisotropic antiferromagnets. However, the full system of non-linear coupled equations, in the replica limit $n \to 0$, has only one stable fixed point, located at

$$u_1^* = u_{12}^* = u_2^* = \frac{1}{32}\frac{\epsilon}{K_4}, \qquad v_1^* = v_{12}^* = v_2^* = 0. \tag{4.15}$$

All the remaining fixed points are unstable, including that one which describes the pure system. As the generalized Gaussian transformation allows the establishment of a contact with the original parameters of the model, we are able to check whether this stable fixed point can be reached from the physical parameter space. In the replica limit $n \to 0$, the coefficients of the quartic isotropic terms in the replica space have well defined signs, whatever the probability distribution $P(D_i)$,

$$16u_{12} = -32u_1 = -8u_2 = (4\beta J S^2 d^2)^2 a^{d-4} \left\{ \left\langle \left(\frac{A_2}{A_0} \right)^2 \right\rangle - \left\langle \frac{A_2}{A_0} \right\rangle^2 \right\} \geq 0. \tag{4.16}$$

The signs of the coordinates of the stable fixed point, which is fully isotropic in the replica space, are incompatible with those fixed by eq. (4.16). Furthermore, these signs are preserved by the renormalization-group transformations, even when all the irrelevant operators are considered in the recursion relations[12,13]. This suggests that the stable fixed point cannot be reached from any initial conditions, in disagreement with the mean-field results. As in the case of random Ising models[14], maybe there is a fixed point of order $\sqrt{\epsilon}$. An investigation of this possibility, however, requires the calculation of the recursion relations up to terms of second order in ϵ.

V. Conclusions

We have presented a detailed mean-field analysis of a classical Heisenberg ferromagnet with the inclusion of random uniaxial single-ion anisotropic terms of the type $-D_i (S_i^z)^2$. The diluted ($D_i = D$, with probability p, and $D_i = 0$, with probability $1-p$, for all sites i) and the pure ($D_i = D$, for all i) models display the same kind of ***T-D*** phase diagram for all values of p. There are two ordered phases (of Ising and XY character) separated by a first-order line which ends at a bicritical point. For a symmetric double-delta distribution ($D_i = D$, with probability p, and $D_i = -D$, with probability 1 – p), there is also an oblique, Heisenberg ordered phase. Depending on the values of p, the ***T-D*** phase diagrams display two distinct multicritical points.

We have also performed some momentum-space renormalization-group calculations to account for the spin fluctuations in the model with short-range interactions. Using the replica trick to average out the quenched random variables, we have obtained a set of coupled non-linear recursion relations to first order in $\epsilon = 4 - d$. In the limit of zero replicas, there is only one stable fixed point, which cannot be reached from physically acceptable initial conditions. Some higher-order calculations are still needed to check the mean-field predictions.

Acknowledgments

M. N. T. acknowledges a fellowship from FAPESP. We acknowledge discussions with Carlos E. I. Carneiro and Carlos S. O. Yokoi. This work was made possible by grants from FAPESP and CNPq.

References

1. C. H. Westphal, D.Sc. Thesis, Instituto de Física, Universidade de São Paulo (1980).
2. C. H. Westphal and C. C. Becerra, J. Phys. C: Solid State Phys. 15, 6221 (1982).
3. K. Katsumata, M. Kobayashi, T. Satõ and Y. Miyako, Phys. Rev. B 19, 2700 (1979).
4. F. Matsubara and S. Inawashiro, J. Phys. Soc. Japan 46, 1740 (1979).
5. R. Harris, M. Plischke and M. J. Zuckermann, Phys. Rev. Lett. 31, 160 (1973).
6. D. S. Fisher, Physica 177 **A,** 84 (1991).
7. A. Aharony, Phys. Rev. B 12, 1038 (1975).
8. D. Mukamel and G. Grinstein, Phys. Rev. B 25, 381 (1982).
9. Y. Y. Goldschmidt, Nuclear Physics B 225 (F59), 123 (1983).
10. K.-S. Liu and M. E. Fisher, J. Low Temp. Phys. 10, 655 (1973).
11. J. M. Kosterlitz, D. R. Nelson and M. E. Fisher, Phys. Rev. B 13, 412 (1976).
12. T. C. Lubensky, Phys. Rev. B **11,** 3573 (1975).
13. A. Aharony, Y. Imry and S.-K. Ma, Phys. Rev. B 13, 466 (1976).
14. A. Aharony, Phys. Rev. B 13, 2092 (1976).